



## Phage display-based discovery of cyclic peptides against the broad spectrum bacterial anti-virulence target CsrA



Valentin Jakob<sup>a, b, 1</sup>, Ben G.E. Zoller<sup>a, b, 1</sup>, Julia Rinkes<sup>a, b</sup>, Yingwen Wu<sup>a, b</sup>, Alexander F. Kiefer<sup>a, b</sup>, Michael Hust<sup>c</sup>, Saskia Polten<sup>c</sup>, Andrew M. White<sup>d</sup>, Peta J. Harvey<sup>d</sup>, Thomas Durek<sup>d</sup>, David J. Craik<sup>d</sup>, Andreas Siebert<sup>e</sup>, Uli Kazmaier<sup>e</sup>, Martin Empting<sup>a, b, \*</sup>

<sup>a</sup> Department of Drug Design and Optimization (DDOP), Helmholtz-Institute for Pharmaceutical Research Saarland (HIPS) - Helmholtz Centre for Infection Research (HZI), Campus E8.1, 66123, Saarbrücken, Germany

<sup>b</sup> Department of Pharmacy, Saarland University, Campus E8.1, 66123, Saarbrücken, Germany

<sup>c</sup> Technische Universität Braunschweig, Institut für Biochemie, Biotechnologie und Bioinformatik, Spielmannstr. 7, 38106, Braunschweig, Germany

<sup>d</sup> ARC Centre of Excellence for Innovations in Peptide and Protein Science, Institute for Molecular Bioscience, The University of Queensland, Brisbane, QLD, 4072, Australia

<sup>e</sup> Institut für Organische Chemie Saarland University Campus C4.2, 66123, Saarbrücken, Germany

### ARTICLE INFO

#### Article history:

Received 26 November 2021

Received in revised form

18 January 2022

Accepted 18 January 2022

Available online 24 January 2022

#### Keywords:

Competitive CsrA inhibition

Disulfide bridges

Disulfide mimetics

Peptides

Phage display

Triazole bridge

### ABSTRACT

Small macrocyclic peptides are promising candidates for new anti-infective drugs. To date, such peptides have been poorly studied in the context of anti-virulence targets. Using phage display and a self-designed peptide library, we identified a cyclic heptapeptide that can bind the carbon storage regulator A (CsrA) from *Yersinia pseudotuberculosis* and displace bound RNA. This disulfide-bridged peptide, showed an IC<sub>50</sub> value in the low micromolar range. Upon further characterization, cyclisation was found to be essential for its activity. To increase metabolic stability, a series of disulfide mimetics were designed and a redox-stable 1,4-disubstituted 1,2,3-triazole analogue displayed activity in the double-digit micromolar range. Further experiments revealed that this triazole peptidomimetic is also active against CsrA from *Escherichia coli* and RsmA from *Pseudomonas aeruginosa*. This study provides an ideal starting point for medicinal chemistry optimization of this macrocyclic peptide and might pave the way towards broad-acting virulence modulators.

© 2022 The Authors. Published by Elsevier Masson SAS. This is an open access article under the CC BY license (<http://creativecommons.org/licenses/by/4.0/>).

## 1. Introduction

For many years, researchers have warned about the antimicrobial resistance (AMR) crisis [1–3]. The rampant spread of multi-drug resistant bacterial pathogens combined with the lack of novel treatment options, especially against Gram-negative species, poses a great threat for our modern healthcare systems [4]. For this reason, the discovery of new anti-infective candidates with novel and innovative mechanisms-of-action are needed. We consider the carbon storage regulator A (CsrA; in some species also called the

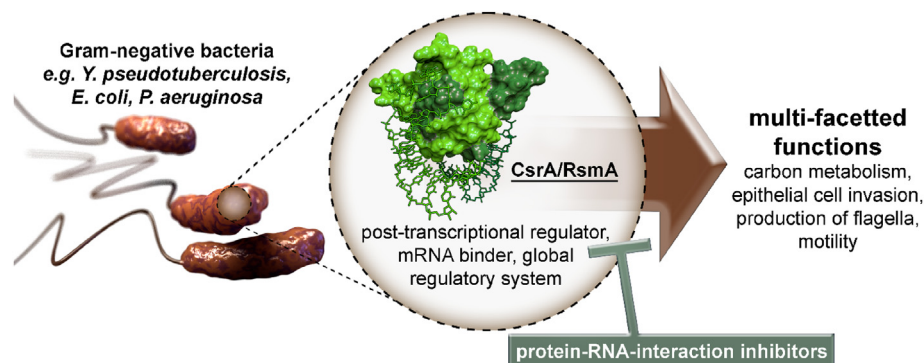
regulator of secondary metabolites, RsmA) [5] as an attractive, yet underexplored, virulence-modulating target [6,7]. It is widespread in Gram-negative pathogens [8] where its sequence and function is highly conserved [9]. Knock-out studies in *Pseudomonas aeruginosa*, *Yersinia pseudotuberculosis* and *Helicobacter pylori* [10] have demonstrated its critical role in bacterial virulence and highlighted its potential as a therapeutic target [11]. The CsrA/RsmA protein is a post-transcriptional regulator [12], that binds and regulates translation of mRNA and, thus exerts pleiotropic effects on the bacterial transcriptome (Fig. 1) [13,14].

Through its mRNA binding activity it is involved in the regulation of quorum sensing [15], motility [16], carbon metabolism [17], peptide uptake *via* cstA [18–20] and biofilm development [21]. To disrupt the function of CsrA/RsmA at the molecular level, protein-RNA interaction inhibitors need to be devised. CsrA usually occurs as a homodimer, with two identical RNA-binding sites [22].

\* Corresponding author. Department of Drug Design and Optimization (DDOP), Helmholtz-Institute for Pharmaceutical Research Saarland (HIPS) - Helmholtz Centre for Infection Research (HZI), Campus E8.1, 66123, Saarbrücken, Germany.

E-mail address: [martin.empting@helmholtz-hzi.de](mailto:martin.empting@helmholtz-hzi.de) (M. Empting).

<sup>1</sup> These authors contributed equally to this work.



**Fig. 1.** CsrA/RsmA as a promising drug target for multi-pathogen virulence modulation by disruption of an essential protein-RNA interaction.

In a previous study using *Yersinia* CsrA and a short piece of RNA that contained the important core binding motif GGA, it was shown that this RNA can be displaced by small molecules [10,23]. In the present work, we sought to find novel lead molecules within the extended Lipinski space (MW between 500 and 1000 Da) [24–26]. These molecules should provide a suitable basis for disrupting macromolecule-macromolecule interactions while still retaining the potential for membrane permeability and oral bioavailability [26,27].

## 2. Materials and methods

### 2.1. Phage display

A detailed description of the experimental procedures used for oligomer design, cloning, library packaging and phage display was previously published as a protocol [28].

In brief, an oligomer was designed, which encodes for a very small peptide library, which has the structure XCXXXXC. There are two fixed cysteine positions in it and X encodes for any amino acid except cysteine. The oligomer was synthesized by Ella Biotech GmbH. This library was cloned into the phagemid pHAL30 [29] where it displays  $2.48 \cdot 10^6$  different peptides. The library was packed into M13K07 phages, which are able to present the peptides on their surface to a protein target.

Under oxidative conditions, the cysteines are forming a macrocycle over the disulfide bond. For selection of potential CsrA binders, phage display was established. For this process, CsrA<sub>-biot\_His<sub>6</sub></sub> was bound to a streptavidin-coated ELISA plate well. After blocking with BSA/milk powder, the pre-selected library, where BSA and streptavidin binders were excluded, was added. Unspecific binders were eliminated with a plate washer (Tecan Hydroflex), where PBS pH 7.4 containing Tween-20 was used. After the third panning round the clones were separated on agar plates. 32 clones were sequenced and checked for plausibility. Criteria for selection were an intact sequence with low tryptophane content and one glutamic acid, while carboxyl groups are beneficial for binding to positively charged surfaces on CsrA. We identified two interesting sequences containing a glutamate residue within the macrocycle. Peptide **1** (*Ac-V-[CSELG]<sub>cyclic</sub>-W-NH<sub>2</sub>*) could be successfully synthesized. Synthesis and macrocyclization of the alternative sequence *Ac-H-[CQEVC]<sub>cyclic</sub>-P-NH<sub>2</sub>* yielded only dimerized product (data not shown). Nevertheless, this finding underscores the potential ionic interaction between the glutamate side chain and basic residues on the protein surface.

CsrA coating amount of the wells, detergent amount in PBS buffer as well as washing stringency with the plate washer were optimized. Before each panning round, the wells were coated with

either 4 µg or 40 µg CsrA<sub>-biot\_His<sub>6</sub></sub>. The better results were obtained with 4 µg. 0 µg CsrA was used as negative control. Before phage elution with trypsin, PBS containing different amounts of Tween-20 (0.05%, 0.1% or 0.2%) was tried to rinse the wells with the plate washer. Since the variation effect was not significant, 0.1% Tween-20 was chosen as the detergent amount. The number of washing cycles, however, had a significant impact on the results. Tested were 2/4/6, 4/8/10 and 10/10/10 washing cycles. The first number corresponds to the number of washing cycles after the first panning round, the second after the second and the third after the third round. The more washing rounds were used, the more sequences containing frame shifts or predominantly hydrophobic amino acids (i.e., more than one tryptophan residues) were found. This was the case for the 4/8/10 and 10/10/10 variant. If, on the other hand, fewer washing cycles were used (2/4/6), a large proportion of pHAL30 origin empty vector containing no peptide encoding sequence was found, but also a few desired peptide sequences as potential binders. Peptide 1 was one of those useful sequences.

### 2.2. Fluorescence polarization assay

The fluorescence polarization assay has been established by Maurer et al. [10]. Fluorescence polarization was recorded using a CLARIOstar microplate reader (BMG LABTECH, Ortenberg, Germany) with an extinction filter at 485 nm and emission filter at 520 nm. Gain adjustment was performed before starting each measurement to achieve maximum sensitivity. The FP values were measured in millipolarization units (mP). The assay was performed two times in duplicates and the IC<sub>50</sub> value was calculated using sigmoidal logistic fit in Origin. Fluorescein-labeled RNA (for *Yersinia* CsrA: 5'-UUCACGGAGAA[flc]; for *E. coli* CsrA: 5'-AGACAAGGAUGU [flc]) was obtained from Sigma Aldrich in HPLC purity. The results of the dose-dependent measurement are shown in Figure S3 and S4.

A 20 mM peptide in DMSO stock solution was diluted with assay buffer (10 mM HEPES, 150 mM NaCl, 0.005% (v/v) Tween-20, ad DEPC-treated H<sub>2</sub>O (RNase free water), pH 7.4) in a way that 3 mM peptide in 15% DMSO was achieved (21 µL 20 mM peptide in DMSO + 119 µL assay buffer). Afterwards, a 1:2 dilution series containing 12 steps was utilized by diluting 70 µL of assay buffer containing 15% DMSO with 70 µL of the peptide in assay buffer with 15% DMSO from this solution (figure S2), starting from 3 mM ended in 1,46 µM. Using a 12-channel pipette, 10 µL of each concentration were transferred to a 384 well microtiter plate (black, flat bottom, Greiner Bio-One) in two replicates and another 10 µL of 1.2 µM (2.4 µM for *E. coli* CsrA) of the corresponding CsrA<sub>-biot-His<sub>6</sub></sub> protein (in assay buffer) were added to each well and quickly centrifuged to be preincubated for 1 h on a Duomax 1030 shaker under light

exclusion. 10  $\mu\text{M}$  fluorescein-labeled RNA (RNAflc) was diluted with assay buffer to a concentration of 45 nM obtaining an end concentration of 15 nM in the assay. After short centrifugation the plate was incubated for 1.5 h on the shaker under light exclusion. The final concentrations in the assay were 400 nM (800 nM for *E. coli* CsrA) CsrA-biot-His<sub>6</sub> (monomer concentration), 5% DMSO, 15 nM RNAflc and 1000  $\mu\text{M}$ –0.49  $\mu\text{M}$  peptide.

Furthermore, a high control was prepared to check for the homogeneity of fluorescence for the complex between protein and RNAflc, a low control to verify the homogeneity of fluorescence for the free RNAflc as well as a blank to exclude any deviation due to the matrix of the assay. For the high control components were 10  $\mu\text{L}$  of 15% DMSO in assay buffer, 10  $\mu\text{L}$  of protein and 10  $\mu\text{L}$  of RNAflc, for the low control corresponding 10  $\mu\text{L}$  of 15% DMSO in assay buffer, 10  $\mu\text{L}$  of assay buffer and 10  $\mu\text{L}$  of RNAflc and the blank consisted of 10  $\mu\text{L}$  of 15% DMSO in assay buffer and two times 10  $\mu\text{L}$  of assay buffer. These three controls were measured in 24-lets.

Moreover, a fluorescence control was performed for the peptides measured to check for the possibility of fluorescence quenching. Therefore, the first component was 10  $\mu\text{L}$  of the dilution series of the corresponding peptide, second component was 10  $\mu\text{L}$  of assay buffer and third component was 10  $\mu\text{L}$  of RNAflc.

Thereby, fluorescence intensity was calculated by determination of the sum of blank corrected based on raw data parallel and perpendicular for the highest concentration on the one hand and for the lowest concentration on the other hand. Afterwards, the average of these two values was determined and the deviation from fluorescence intensity to the average value should be under 20% for no fluorescence quenching. This was the reason why the 1000  $\mu\text{M}$  and 500  $\mu\text{M}$  value was not included in the assay for **3d** and **5a**.

### 2.3. Microscale thermophoresis assay (MST)

The MST assay was performed according to the protocol of the Monolith NT™ His-Tag labelling Kit RED-tris-NTA and was used for Peptide **1** only. The *Yersinia* CsrA-biot-His<sub>6</sub> monomer concentration was adjusted with assay buffer (10 mM HEPES, 150 mM NaCl, 0.005% (v/v) Tween-20, ad DEPC-treated H<sub>2</sub>O (RNase free water), pH 7.4) to 200 nM in a volume of 100  $\mu\text{L}$ , mixed with 100  $\mu\text{L}$  100 nM dye (Nano RED) and incubated for 30 min in the dark at room temperature. The sample was centrifuged for 10 min at 4 °C and 15000 g. This was the ready-labeled protein. A 20 mM peptide DMSO stock solution was diluted with assay buffer to 2 mM, that the highest end concentration in the assay was 1000  $\mu\text{M}$  with 5% DMSO. 20  $\mu\text{L}$  of the 2 mM peptide was transferred into a first PCR tube and 10  $\mu\text{L}$  of assay buffer containing 10% DMSO was transferred into each next PCR tube 2–16. For the serial dilution series of the peptide, 10  $\mu\text{L}$  of the ligand from tube 1 were transferred to tube 2 with a pipette and mixed by pipetting up-and-down several times. The procedure was repeated for tube 3–16 and 10  $\mu\text{L}$  from tube 16 were discarded. Finally, 10  $\mu\text{L}$  of the labeled protein were added to each PCR tube, mixed with a pipette and incubated in the dark for 45 min. All 16 dilutions were loaded into Monolith NT™ Standard Capillaries and measured in the Monolith NT.115™ device with 60% excitation power and 40% MST power. The protein concentration in the assay was 50 nM. The assay was performed three times in duplicates and the  $K_d$  value of  $10.5 \pm 1.4 \mu\text{M}$  was calculated using sigmoidal logistic fit in Origin. The results from the MST assay for peptide **1** can found in [figure S5](#).

### 2.4. Peptide synthesis and macrocyclization

#### 2.4.1. General information

All resins were purchased from Rapp Polymere. The azide/alkyne building blocks Fmoc-L-azidoalanine (Fmoc-Aza-OH), Fmoc-

L-propargylglycine (Fmoc-Pra-OH) and Fmoc-L-homoazidoalanine (Fmoc-Aha-OH) were purchased from Carl Roth VG. Fmoc-Val-OH, Fmoc-Ala-OH, Fmoc-Glu(OtBu)-OH, Fmoc-Leu-OH and Fmoc-Cys(Trt)-OH were purchased from Novabiochem. Fmoc-Ser(tBu)-OH was purchased from TCI.

#### 2.4.2. General Fmoc-SPPS procedure

Most peptides were synthesized manually via solid phase peptide synthesis (SPPS) using Fmoc chemistry. The resin was swollen for 30 min in DMF. For Fmoc deprotection piperidine/DMF (1:4, v:v) was added and shaken for 5 min, twice. It was then washed five times with DMF followed by the second round of adding piperidine/DMF (1:4) with incubating 5 min on a shaker. It was washed five times with DMF, five times with DCM and again one time with DMF. We used double coupling for each amino acid. The amino acid (4.0 eq.) was solved in DMF together with 3.9 eq 3-[Bis(dimethylamino)methyl]methyl] -3H-benzotriazol-1-oxide hexafluorophosphate (HBTU) followed by adding 8.0 eq. *N*-Ethyl-*N*-(propan-2-yl)propan-2-amine (DIPEA). This solution was pre-activated for 5 min on a shaker. The activated solution was added to the resin and incubated for 1 h on a shaker. After washing five times with DMF, it was added an activated amino acid/HBTU/DIPEA/DMF solution again and incubated 1 h on a shaker. The resin was washed five times with DMF and five times with DCM. This was followed by two deprotection cycles and two coupling cycles of the next amino acid.

#### 2.4.3. General acetylation procedure

For Acetylation, DMF/DIPEA/AC<sub>2</sub>O (12:8:5, v:v:v) was added to the resin and shaken for 0.5 h. Then it was washed five times with DMF, five times with DCM and again one time with DMF.

#### 2.4.4. General cleavage procedure

For protein cleavage from the solid support and removal of the side chain protecting groups a cleavage cocktail containing trifluoroacetic acid (TFA)/triisopropylsilane (TIS)/H<sub>2</sub>O/anisole (95:2:2:1, v:v:v) with a spatula tip of dithiothreitol (DTT) was added to the resin and incubated 2.5–3.0 h on a shaker. The liquid was collected and TFA was removed under reduced pressure, followed by precipitation with cold (–20 °C) methyl *tert*-butyl ether (MTBE). The crude peptide was gained by centrifugation (4600 rpm, 4 °C, 10 min) followed by MTBE washing (3x) and repeated centrifugation.

#### 2.4.5. General cyclisation procedure

For disulfide cyclisation the crude lyophilized peptide was dissolved in H<sub>2</sub>O/ACN (1:1, v:v) with a concentration of 1 mg peptide per 1 mL solvent and 1–3% DMSO was added. The pH was adjusted to 7.7 using 1 M aq. ammonium carbonate solution. The solution was stirred for 1–4 days. The reaction was monitored by LC-MS.

#### 2.4.6. General preparative HPLC procedure

The purification was done with a DIONEX UltiMate 3000 UHPLC<sup>+</sup> focused (Thermo Scientific), containing pump, diode array detector, and automated fraction collector. We used a VP 250/10 NUCLEODUR C18 Gravity, 5  $\mu\text{m}$  (Macherey-Nagel) column with a gradient from 10 to 50% solvent B over 25 min (solvent A: H<sub>2</sub>O (0.05% formic acid), solvent B: ACN (0.05% formic acid)) and a 5 mL/min flowrate. Pure fractions were checked by LC-MS, combined and lyophilized.

## 3. Results and discussion

### 3.1. Phage display

We devised a strategy to screen a library of disulfide-constrained heptapeptides covering a mass range between 548

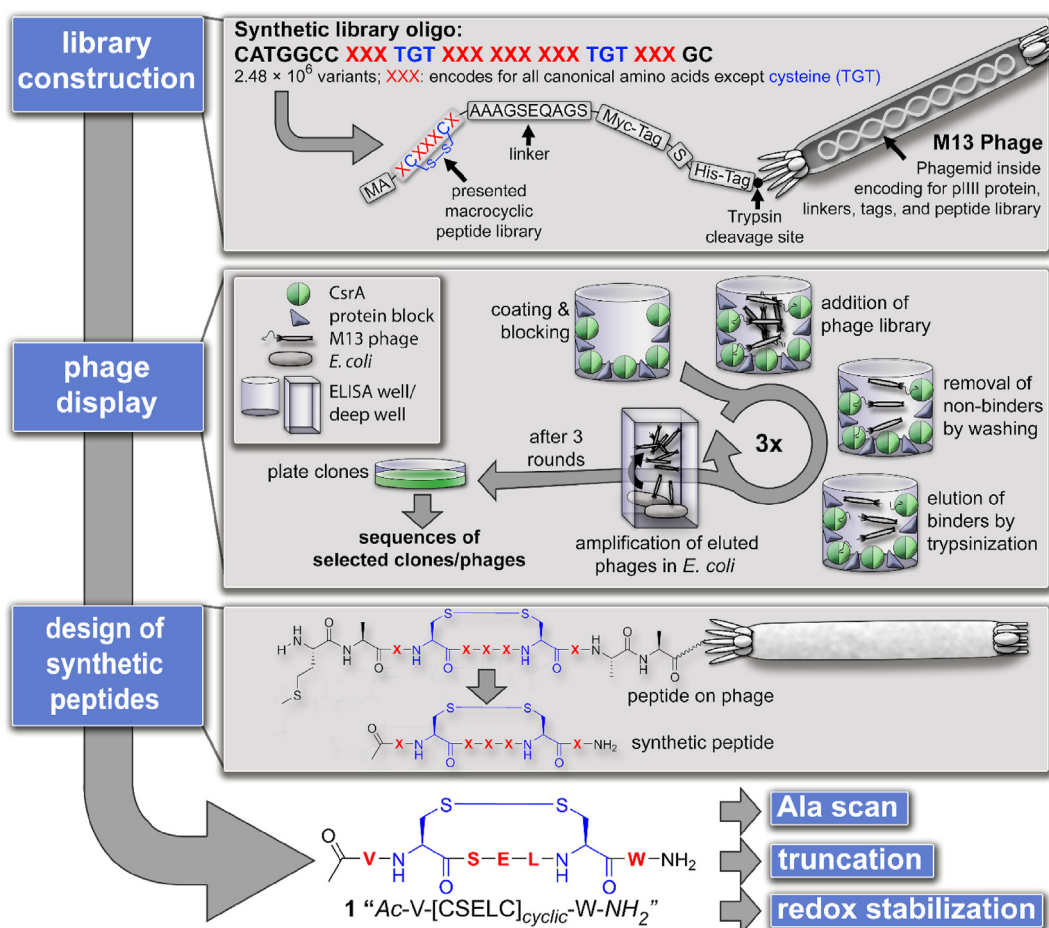
and 1193 Da via phage display (Scheme 1) [28]. The use of phage-encoded libraries displaying millions of compound variants [30] has proven to be an excellent method for finding novel binders for several targets [31]. An important example is the search for small antibody fragments, so called single-chain variable fragments (scFvs) for any desired target [32,33]. Phage display can also be transferred to libraries encoding for short peptides [31,34]. This method allows screening of whole peptide libraries to find potential binders for a given target [35].

Our self-designed phage library encodes for a peptide library with the general structure XCXXXCX ( $2.48 \cdot 10^6$  variants) [28]. It contains two cysteine residues at fixed positions, which form a disulfide bond under oxidative conditions; X encodes for any amino acid except cysteine. This design provides the means to identify very small peptides with a mass range of around 550–1200 Da that are rigidified by a well-defined macrocyclization motif. We screened this library against immobilized *Yersinia* CsrA (biotinylated and His-tagged CsrA construct CsrA<sub>biot</sub>His<sub>6</sub>; more details on phage display and CsrA expression can be seen in Supporting Information and a published protocol) bound to a streptavidin-coated ELISA well. After three rounds of panning, phage binding with high affinity were separated on agar plates. After sequencing of 32 clones, we identified one sequence as a

potential CsrA binder. The criteria for selection were intact sequences and avoidance of a high tryptophan content (more than two Trp), which usually leads to unspecific binding [36]. Notably, the selected sequence contained a glutamic acid residue - a feature we deemed plausible as anionic carboxyl groups should be of benefit for binding the positively charged surface of CsrA possessing a high content of basic amino acids.

### 3.2. First evaluation of peptidic hit

This peptidic hit (1) was synthesized by solid phase peptide synthesis (SPPS) in disulfide-cyclized, *N*-terminally acetylated and C-terminally amidated form. These modifications were chosen because the sequence is presented within a peptide backbone extending beyond its *N*- and C-termini on the phage during the panning experiment. The peptide was characterized by LC-MS, HRMS and NMR (Supporting Information). Using an established fluorescence polarization assay [10] (2.4), peptide 1 was tested for its ability to displace mRNA from CsrA. In this assay a fluorescein (flc)-labeled RNA (5'-UUCACGGAGAA[flc]) and CsrA<sub>biot</sub>His<sub>6</sub> were used to probe the protein-RNA interaction. The labeled RNA was successfully displaced by peptide 1 with an IC<sub>50</sub> value in the micromolar range ( $6.9 \pm 1.3 \mu\text{M}$ , Fig. 2). This peptide amongst the



**Scheme 1.** Phage display-based selection process from library design to peptide hit identification. Library construction: An oligomer was constructed to code for the subsequent peptide library. After cloning and packaging in M13 phage, genotype and phenotype are coupled by presenting the encoded peptide including tags and linkers simultaneously. Phage display: The peptide phage library was used in the panning process, in which the enrichment of potential CsrA binders is achieved. Sequences of the bound peptides were identified by sequencing the coding phage gene. Design of synthetic peptides: Representation of a phage from panning to which a general library peptide including peptide backbone is linked, compared to the synthesized peptides. Here, *N*-terminal acetylation and C-terminal amidation simulate the peptide backbone. Furthermore: A representation of the selected peptide 1 is given, which was characterized in more detail as a "hit" in the context of this paper.



most potent compounds discovered against CsrA to date and is readily synthetically accessible. Previously identified natural products such as MM14 and tubulysin Ar-672, have shown similar potency ( $4 \pm 1 \mu\text{M}$  and  $11 \pm 1 \mu\text{M}$ , respectively) [10], but are much more challenging to synthesize.

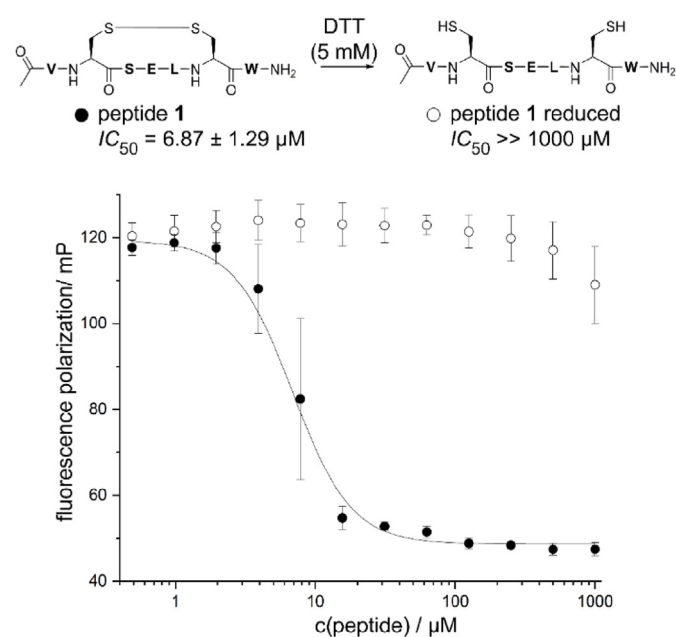
When the assay was conducted in the presence of 5 mM DTT, peptide **1** lost its activity almost completely. Under these conditions the disulfide bond is reduced and the macrocycle linearized. Thus, we concluded that the conformational constraint induced by the disulfide bond is essential for activity. This observation also supports a conformation-specific (structure-dependent) interaction between the peptide and CsrA. Additionally, a microscale thermophoresis (MST) assay was performed with peptide **1** and CsrA<sub>-biot\_His<sub>6</sub></sub> yielding a  $K_d$  of  $10.5 \pm 1.4 \mu\text{M}$  (2.5). This assay further supports a direct specific interaction between the peptide and CsrA.

### 3.3. Alanine scan and truncation

To gain further insights into the underlying structure-activity relationship (SAR) of peptide **1** we synthesized an array of derivatives by Fmoc-SPPS, oxidized them with DMSO and tested for inhibitory activity in the fluorescence polarization assay. The resulting  $IC_{50}$  values are listed in Table 1.

To investigate the importance of the *N*-terminal acetylation as well as the *C*-terminal amide, peptides **2a** and **2b** were synthesized, respectively. We observed slightly increased  $IC_{50}$  values ( $27.6 \pm 4.0 \mu\text{M}$  and  $17.4 \pm 2.0 \mu\text{M}$ , respectively) indicating that both modifications contribute to the overall affinity of peptide **1**. To identify possible interaction hotspots, an alanine scan of peptide **1** was performed.

As expected, activity was abolished when both cysteine residues were replaced by alanine (**3a**) corroborating our earlier findings when using DTT to linearize peptide **1** (Fig. 1). Similarly, when Ser3 (**3c**) or Trp7 (**3f**) were changed to alanine, dramatic losses of activity



**Fig. 2.** Displacement of RNAflc from CsrA<sub>-biot\_His<sub>6</sub></sub> with peptide **1** and its reduced derivative measured via fluorescence polarization. Data shown are from two independent experiments measured in duplicate and were fitted to a sigmoidal logistic, Levenberg Marquardt inhibition model (solid line). The results of peptide **1** (filled circles) as well as peptide **1** in the presence of 5 mM DTT in the assay are shown (open circles).

**Table 1**

Peptides **1–4b** with corresponding  $IC_{50}$  values obtained from the fluorescence polarization assay and their activity relative to peptide **1**.

Entry	Sequence <sup>a</sup>	$IC_{50}/\mu\text{M}^b$ <i>Y. pseudotuberculosis</i>	Relative activity <sup>c</sup>
<b>1</b>	Ac-V-[CSELC] <sub>cyclic</sub> -W-NH <sub>2</sub>	$6.9 \pm 1.3$	1
<b>2a</b>	<b>H</b> -V-[CSELC] <sub>cyclic</sub> -W-NH <sub>2</sub>	$27.6 \pm 4.0$	0.25
<b>2b</b>	Ac-V-[CSELC] <sub>cyclic</sub> -W- <b>OH</b>	$17.4 \pm 2.0$	0.4
<b>3a</b>	Ac-VASELAW-NH <sub>2</sub>	$\gg 1000$	–
<b>3b</b>	Ac-A-[CSELC] <sub>cyclic</sub> -W-NH <sub>2</sub>	$114 \pm 8$	0.06
<b>3c</b>	Ac-V-[CAELC] <sub>cyclic</sub> -W-NH <sub>2</sub>	$>1000$	–
<b>3d</b>	Ac-V-[CSALC] <sub>cyclic</sub> -W-NH <sub>2</sub>	$22.8 \pm 0.7$	0.3
<b>3e</b>	Ac-V-[CSEAC] <sub>cyclic</sub> -W-NH <sub>2</sub>	$57.9 \pm 2.1$	0.12
<b>3f</b>	Ac-V-[CSELC] <sub>cyclic</sub> -A-NH <sub>2</sub>	$>500$	–
<b>4a</b>	Ac- -[CSELC] <sub>cyclic</sub> -W-NH <sub>2</sub>	$128 \pm 4$	0.05
<b>4b</b>	Ac-V-[CSELC] <sub>cyclic</sub> - -NH <sub>2</sub>	$\gg 1000$	–

<sup>a</sup> Differences relative to peptide **1** are shown in bold or as “–” for deletions. Each peptide is disulfide-cyclized (except **3a**) over the cysteines.

<sup>b</sup> Standard error of the sigmoidal curve fit is given (two independent experiments, measured in duplicates).

<sup>c</sup> Relative activity for a peptide **x** is given as the ratio  $IC_{50}(\text{peptide } \mathbf{1})/IC_{50}(\text{peptide } \mathbf{x})$ .

were observed. Therefore, the interactions mediated by the serine and tryptophan sidechains are essential hotspots for high affinity. Furthermore, the Ala-scan allowed us to conclude that substitution of residues Val1 (**3b**), Glu4 (**3d**) or Leu5 (**3e**) has a less pronounced effect on activity, showing  $IC_{50}$  values of  $114 \pm 8 \mu\text{M}$ ,  $22.8 \pm 0.7 \mu\text{M}$ , and  $57.9 \pm 2.1 \mu\text{M}$ , respectively. In the case of the Glu4Ala mutation, this result was surprising. CsrA is an RNA-binding protein possessing a positively charged surface area due to an abundance of lysine and arginine residues. Hence, the presence of the carboxylic acid function in peptide **1** hinted at a potential salt bridge as an important contribution to affinity. If the proposed ionic interaction between Glu4 and the basic amino acid sidechains of CsrA was optimally positioned, a dramatic loss of affinity would have been expected for compound **3d**. As this was not the case, this position should be investigated in more detail in future optimization efforts.

Two truncated versions were tested for inhibitory activity to check whether further reduction in size is possible. A version without Val1 (**4a**) had an  $IC_{50}$  of  $128 \pm 4 \mu\text{M}$ , which is comparable to the value obtained for the Val1Ala mutant, **3b** ( $114 \pm 8 \mu\text{M}$ ). If tryptophan is omitted (**4b**), the activity in the measured concentration range is completely lost and in line with our findings with the Trp7Ala mutant (**3f**). Hence, we conclude that the complete seven amino acid sequence is required for high activity.

### 3.4. Disulfide replacement by triazole bridge

In a final step, we sought to protect peptide **1** from reductive linearization, which we consider essential for achieving intracellular activity. To this end, we made use of the “triazole bridge” approach [37] and replaced the cysteine residues with non-natural amino acids bearing alkyne and azide functions in their sidechain for facile click chemistry-based macrocyclization [38–40]. Notably, this strategy provides selective access to either a 1,4-disubstituted or 1,5-disubstituted bridging motif depending on whether copper(I)- or ruthenium(II)-catalyzed azide-alkyne cycloaddition is applied (abbreviated CuAAC or RuAAC, respectively). This method had recently been used, with great success, by the groups of Tomassi et al. [41], Tala et al. [42] and Pacifico et al. [43] to generate redox stable derivatives of disulfide bridge containing peptides. By this means, several different triazole-bridged peptides were generated (Table 2). The linear precursor peptides were synthesized using commercially available building blocks Fmoc-protected propargylglycine (Fmoc-Pra-OH) and Fmoc-protected azidoalanine

(Fmoc-Aza-OH) or Fmoc-protected azidohomoalanine (Fmoc-Aha-OH). In-solution CuAAC macrocyclization of the unprotected peptides in separate reactions delivered three 1,4-disubstituted 1,2,3-triazole variants (**5a–5c**), which were characterized by LC-MS, HRMS and NMR (Supporting Information) and tested in the fluorescence polarization assay (Table 2). **5a**, originating from an azidoalanine-bearing precursor, showed an  $IC_{50}$  of  $35.3 \pm 0.6 \mu\text{M}$ , which correlates to a moderate 5-fold reduction in potency compared to the disulfide counterpart **1**. Installing an elongated macrocyclization motif by using azidohomoalanine instead (**5c**) leads to a further reduction of activity ( $76.0 \pm 3.3 \mu\text{M}$ ). Changing the orientation of the triazole ring by switching positions of the propargylglycine and azidoalanine residues (**5b**) resulted in an  $IC_{50}$  of  $92.8 \pm 4.0 \mu\text{M}$ .

Previous work on a 14-amino acid, backbone cyclic protease inhibitor peptide SFTI-1, demonstrated the utility of 1,5-disubstituted bridging motifs, which are installed via RuAAC in solution or on resin [37,44]. In the case of our current CsrA-RNA-interaction inhibitor **1**, this strategy was surprisingly not beneficial. Macrocytic peptide **6a** achieved only an  $IC_{50}$  of  $178 \pm 12 \mu\text{M}$ . If the azidoalanine in position 2 was replaced by azidohomoalanine (**6b**), the  $IC_{50}$  value increased even further to  $337 \pm 34 \mu\text{M}$ . Finally, exchanging the positions of Aha and Pra (**6c**) did not show any significant difference in comparison to **6b** ( $IC_{50} = 309 \pm 15 \mu\text{M}$ ).

To demonstrate the potential for a broader anti-Gram-negative activity we tested peptide **1** and our triazole-stabilized derivatives against the *E. coli* and the *Pseudomonas aeruginosa* homologs of CsrA (RsmA, Table 2). Surprisingly, disulfide-cyclized inhibitor **1** showed a reduced activity ( $IC_{50}$  (*E. coli*) =  $182 \pm 67 \mu\text{M}$ ,  $IC_{50}$  (*P. aeruginosa*) =  $272 \pm 68 \mu\text{M}$ ), while the 1,4-disubstituted triazoles **5a**, **5b** and **5c** now outperformed the parent peptide ( $IC_{50}$  (*E. coli*) =  $4.9 \pm 0.9 \mu\text{M}$ ,  $6.8 \pm 1.5 \mu\text{M}$ , and  $3.4 \pm 0.6 \mu\text{M}$ ,  $IC_{50}$  (*P. aeruginosa*) =  $20 \pm 5.4 \mu\text{M}$ ,  $22.8 \pm 5.0 \mu\text{M}$ , and  $30.2 \pm 3.2 \mu\text{M}$ ). The 1,5-disubstituted congeners again showed reduced activity compared to their 1,4-counterparts, albeit still being more active than the disulfide compound **1**. Considering the high sequence identity between CsrA from *Yersinia* and *E.coli* (95%) [45], it is fair to assume that this finding provides evidence for the potential site of interaction of the macrocyclization motif for our inhibitor scaffold. The only differences in amino acid sequence between the

*Y. pseudotuberculosis* and *E. coli* proteins are at distinct residues of the C-terminus, including Pro58Gln, Thr59Ser, and Thr60Ser, respectively (see sections regarding protein expression in the Supporting Information). This region is also close to the protein-RNA-interaction interface (Fig. 3). Hence, we hypothesize that the inhibitor scaffold covers an area encompassing interactions to both sites (C-terminus and RNA-binding site). Unfortunately, attempts to co-crystallize the peptide with CsrA have not been successful to date. To gain access to structural information, we solved the structure of peptide **1** by NMR (PDB ID 7M7X, BMRB ID 30895, Fig. 3a and Supporting Information). With this ligand structure ensemble in hand we performed a docking experiment based on a *Y. pseudotuberculosis* CsrA homology model derived from a protein-RNA complex determined by NMR [46]. The result of the docking experiment is shown in Fig. 3b (see also Supporting Information). The binding pose of peptide **1** is in line with the SAR derived via the Ala-scan and truncation experiments. For example, the side chains of “hot spot” residues Ser3 and Trp7 form key contacts with Lys38 and Val40, while the other residues are primarily involved in backbone-based interactions (Fig. 3c). Although this pose will need further validation in future studies, it provides a basis for explaining the observed differences between *Y. pseudotuberculosis* and *E. coli* CsrA. We hypothesize that the differences in activities seen for compounds in Table 2 are potentially resulting from the Pro58Gln mutation changing the C-terminal interaction site from a rather hydrophobic environment to a more polar one, which might favor the hydrogen acceptor functions of the triazole. Implementation of a 1,5-motif (6a – 6c), however, could result in steric clashes between the ligand and the protein target rendering them less effective in this scenario.

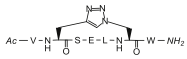
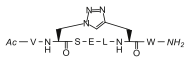
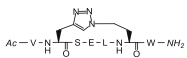
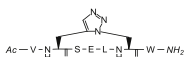

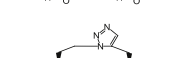
Along similar lines, the decreased sequence identity between CsrA (*Y. pseudotuberculosis*, *E. coli*) and RsmA (*P. aeruginosa*) of 85% (*E. coli* – *P. aeruginosa*) or 86% (*Y. pseudotuberculosis* – *P. aeruginosa*) arising again mainly at the C-terminal end might explain the different SAR observation made (Table 2, Supporting Information).

#### 4. Conclusion

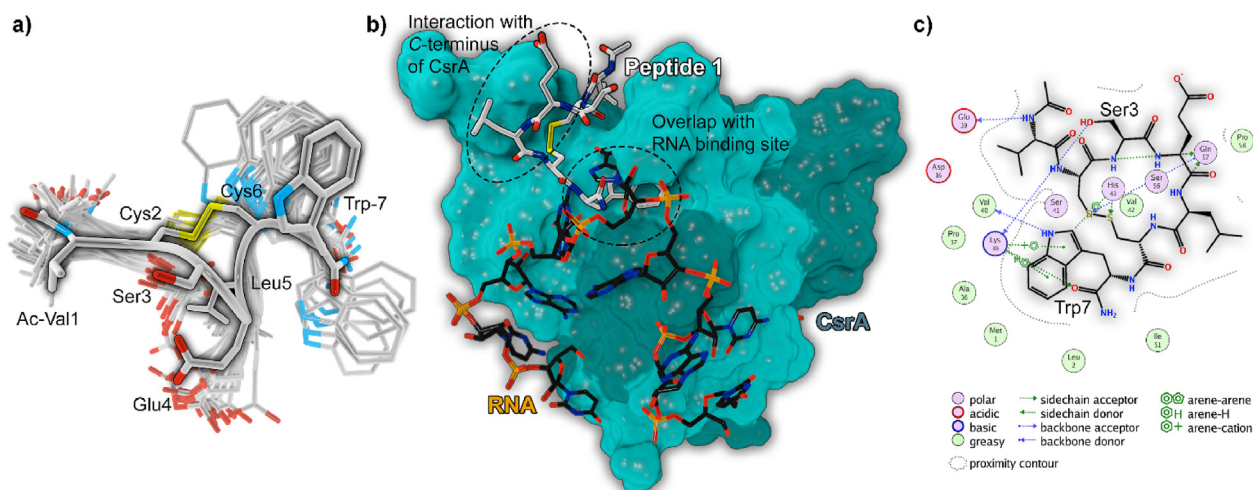
In summary, we have shown that the 1,4-disubstituted triazole bridging motif established in **5a** is a suitable disulfide replacement that is active against *Y. pseudotuberculosis*, *E. coli* and *P. aeruginosa*

**Table 2**

Peptide **1** and triazole-bridged variants **5a–6c** with corresponding  $IC_{50}$  values obtained for *Yersinia* and *E. coli* CsrA and RsmA from *P. aeruginosa* from a fluorescence polarization assay.

Entry	Sequence	$IC_{50}/\mu\text{M}^a$ <i>Yersinia</i>	$IC_{50}/\mu\text{M}^a$ <i>E. coli</i>	$IC_{50}/\mu\text{M}^a$ <i>P. aeruginosa</i>
<b>1</b>	Ac-V-[CSEL <sub>C</sub> ] <sub>cyclic</sub> -W-NH <sub>2</sub>	6.9 ± 1.3	182 ± 67	272 ± 68
<b>5a</b>		35.3 ± 0.6	4.9 ± 0.9	20 ± 5.4
<b>5b</b>		92.8 ± 4.0	6.8 ± 1.5	22.8 ± 5.0
<b>5c</b>		76.0 ± 3.3	3.4 ± 0.6	30.2 ± 3.2
<b>6a</b>		178 ± 12	48.1 ± 16	50 ± 15
<b>6b</b>		337 ± 34	51.6 ± 27.1	44.4 ± 9.7
<b>6c</b>		309 ± 15	83.4 ± 47.1	37 ± 17

<sup>a</sup> Standard error of the sigmoidal curve fit is given (two independent experiments, measured in duplicate).



**Fig. 3.** *In silico* analysis of the peptide-CsrA interaction. a) Overlay of 20 NMR-derived solution structures of peptide 1 (PDB ID 7M7X, BMRB ID 30895) showing the peptide backbone as a tube and highlighting conformer 1 (entry 1 in pdb) for clarity. b) Depiction of docking-derived interaction hypothesis highlighting key interaction sites. Carbons of peptide 1 are shown in white and RNA carbons in black. Surface of the two CsrA chains shown in light cyan and dark cyan. c) 2D interaction profile of binding hypothesis for peptide 1. "Hot spot" residues identified via Ala-scan (Ser3 and Trp7) are indicated.

CsrA. In combination with our phage display-based screening methodology, we have provided a generic approach towards the identification, initial qualification, and subsequent redox-protection of short macrocyclic peptides as protein-RNA-interaction inhibitors. The phage display methodology proved to be a rapid approach towards identification of the first macrocyclic peptide able to disrupt the CsrA-RNA interaction. The starting scaffold peptide **1** was thoroughly characterized by fluorescence polarization-based functional activity tests as well as MST-based protein binding assay. Exchanging the disulfide bond with a redox stable 1,2,3-triazole bridge gave us active non-natural derivatives suitable for future cell-based assays. Contrary to previous studies, we have observed that in the current system the synthetically easier accessible 1,4-disubstituted 1,2,3-triazole was the superior disulfide mimic showing an  $IC_{50}$  value in the 2-digit micromolar range. Based on NMR-based solution structure determination of the native peptide sequence and docking experiments structure-guided optimization can now be attempted. This novel scaffold serves as a suitable starting point for the generation of high potency CsrA inhibitors, also because it is applicable against CsrA from further bacterial species with high medical need (*P. aeruginosa*).

#### Author contribution

The author contributions can be found in the supporting information.

#### Declaration of competing interest

The authors declare that they have no known competing financial interests or personal relationships that could have appeared to influence the work reported in this paper.

#### Acknowledgments

This work is supported by the Deutsche Forschungsgemeinschaft (DFG) through "RESIST - Resolving Infection Susceptibility" cluster of excellence (EXC 2155). Work in DJCs lab on cyclic peptides is supported by the Australian Research Council (CE200100012). We thank Prof. Dr. Tony Romeo for sending us the plasmid for *E. coli* CsrA expression.

#### Appendix A. Supplementary data

Supplementary data to this article can be found online at <https://doi.org/10.1016/j.ejmech.2022.114148>.

#### References

- [1] M. Jemal, T. Deress, T. Belachew, Y. Adem, Antimicrobial resistance patterns of bacterial isolates from blood culture among HIV/AIDS patients at felege hiwot referral hospital, northwest Ethiopia, *Internet J. Microbiol.* 2020 (2020) 8893266, <https://doi.org/10.1155/2020/8893266>.
- [2] H. Inoue, R. Minghui, Antimicrobial resistance: translating political commitment into national action, *Bull. World Health Organ.* 95 (2017) 242, <https://doi.org/10.2471/BLT.17.191890>.
- [3] Z. Kmiotowicz, Few novel antibiotics in the pipeline, WHO warns, *BMJ* 358 (2017) j4339, <https://doi.org/10.1136/bmj.j4339>.
- [4] S. Vasoo, J.N. Barreto, P.K. Tosh, Emerging issues in gram-negative bacterial resistance: an update for the practicing clinician, *Mayo Clin. Proc.* 90 (2015) 395–403, <https://doi.org/10.1016/j.mayocp.2014.12.002>.
- [5] Y. Irie, M. Starkey, A.N. Edwards, D.J. Wozniak, T. Romeo, M.R. Parsek, *Pseudomonas aeruginosa* biofilm matrix polysaccharide Psl is regulated transcriptionally by RpoS and post-transcriptionally by RsmA, *Mol. Microbiol.* 78 (2010) 158–172, <https://doi.org/10.1111/j.1365-2958.2010.07320.x>.
- [6] A.M. Nuss, A.K. Heroven, P. Dersch, RNA regulators: formidable modulators of *Yersinia* virulence, *Trends Microbiol.* 25 (2017) 19–34, <https://doi.org/10.1016/j.tim.2016.08.006>.
- [7] F.M. Barnard, M.F. Loughlin, H.P. Fainberg, M.P. Messenger, D.W. Ussery, P. Williams, P.J. Jenks, Global regulation of virulence and the stress response by CsrA in the highly adapted human gastric pathogen *Helicobacter pylori*, *Mol. Microbiol.* 51 (2004) 15–32, <https://doi.org/10.1046/j.1365-2958.2003.03788.x>.
- [8] A.H. Potts, C.A. Vakulskas, A. Pannuri, H. Yakhnin, P. Babitzke, T. Romeo, Global role of the bacterial post-transcriptional regulator CsrA revealed by integrated transcriptomics, *Nat. Commun.* 8 (2017) 1596, <https://doi.org/10.1038/s41467-017-01613-1>.
- [9] E.R. Morris, G. Hall, C. Li, S. Heeb, R.V. Kulkarni, L. Lovelock, H. Silistre, M. Messina, M. Cámara, J. Emsley, P. Williams, M.S. Searle, Structural rearrangement in an RsmA/CsrA ortholog of *Pseudomonas aeruginosa* creates a dimeric RNA-binding protein, *RsmN*, *Structure* 21 (2013) 1659–1671, <https://doi.org/10.1016/j.str.2013.07.007>.
- [10] C.K. Maurer, M. Fruth, M. Empting, O. Avrutina, J. Hoßmann, S. Nadmid, J. Gorges, J. Herrmann, U. Kazmaier, P. Dersch, R. Müller, R.W. Hartmann, Discovery of the first small-molecule CsrA-RNA interaction inhibitors using biophysical screening technologies, *Future Med. Chem.* 8 (2016) 931–947, <https://doi.org/10.4155/fmc-2016-0033>.
- [11] G. Sharma, S. Sharma, P. Sharma, D. Chandola, S. Dang, S. Gupta, R. Gabrani, *Escherichia coli* biofilm: development and therapeutic strategies, *J. Appl. Microbiol.* 121 (2016) 309–319, <https://doi.org/10.1111/jam.13078>.
- [12] J. Timmermans, L. van Melder, Post-transcriptional global regulation by CsrA in bacteria, *Cell, Mol. Life Sci.* 67 (2010) 2897–2908, <https://doi.org/10.1007/s00018-010-0381-z>.
- [13] E. van Assche, S. van Puyvelde, J. Vanderleyden, H.P. Steenackers, RNA-binding



- proteins involved in post-transcriptional regulation in bacteria, *Front. Microbiol.* 6 (2015) 141, <https://doi.org/10.3389/fmicb.2015.00141>.
- [14] N.A. Sabnis, H. Yang, T. Romeo, Pleiotropic regulation of central carbohydrate metabolism in *Escherichia coli* via the gene *csrA*, *J. Biol. Chem.* 270 (1995) 29096–29104, <https://doi.org/10.1074/jbc.270.49.29096>.
- [15] H. Yakhnin, C.S. Baker, I. Berezin, M.A. Evangelista, A. Rassin, T. Romeo, P. Babitzke, CsrA represses translation of *sdiA*, which encodes the N-acylhomoserine-L-lactone receptor of *Escherichia coli*, by binding exclusively within the coding region of *sdiA* mRNA, *J. Bacteriol.* 193 (2011) 6162–6170, <https://doi.org/10.1128/JB.05975-11>.
- [16] B.L. Wei, A.M. Brun-Zinkernagel, J.W. Simecka, B.M. Prüss, P. Babitzke, T. Romeo, Positive regulation of motility and *flhDC* expression by the RNA-binding protein CsrA of *Escherichia coli*, *Mol. Microbiol.* 40 (2001) 245–256, <https://doi.org/10.1046/j.1365-2958.2001.02380.x>.
- [17] M.Y. Liu, G. Gui, B. Wei, J.F. Preston, L. Oakford, U. Yüksel, D.P. Giedroc, T. Romeo, The RNA molecule CsrB binds to the global regulatory protein CsrA and antagonizes its activity in *Escherichia coli*, *J. Biol. Chem.* 272 (1997) 17502–17510, <https://doi.org/10.1074/jbc.272.28.17502>.
- [18] Y. Tan, Z.-Y. Liu, Z. Liu, H.-J. Zheng, F.-L. Li, Comparative transcriptome analysis between *csrA*-disruption *Clostridium acetobutylicum* and its parent strain, *Mol. Biosyst.* 11 (2015) 1434–1442, <https://doi.org/10.1039/c4mb00600c>.
- [19] J.E. Schultz, A. Matin, Molecular and functional characterization of a carbon starvation gene of *Escherichia coli*, *J. Mol. Biol.* 218 (1991) 129–140, [https://doi.org/10.1016/0022-2836\(91\)90879-B](https://doi.org/10.1016/0022-2836(91)90879-B).
- [20] A.K. Dubey, C.S. Baker, K. Suzuki, A.D. Jones, P. Pandit, T. Romeo, P. Babitzke, CsrA regulates translation of the *Escherichia coli* carbon starvation gene, *cstA*, by blocking ribosome access to the *cstA* transcript, *J. Bacteriol.* 185 (2003) 4450–4460, <https://doi.org/10.1128/jb.185.15.4450-4460.2003>.
- [21] D.W. Jackson, K. Suzuki, L. Oakford, J.W. Simecka, M.E. Hart, T. Romeo, Biofilm formation and dispersal under the influence of the global regulator CsrA of *Escherichia coli*, *J. Bacteriol.* 184 (2002) 290–301, <https://doi.org/10.1128/jb.184.1.290-301.2002>.
- [22] A.K. Dubey, C.S. Baker, T. Romeo, P. Babitzke, RNA sequence and secondary structure participate in high-affinity CsrA-RNA interaction, *RNA* 11 (2005) 1579–1587, <https://doi.org/10.1261/rna.2990205>.
- [23] X. Ren, R. Zeng, M. Tortorella, J. Wang, C. Wang, Structural insight into inhibition of CsrA-RNA interaction revealed by docking, molecular dynamics and free energy calculations, *Sci. Rep.* 7 (2017) 14934, <https://doi.org/10.1038/s41598-017-14916-6>.
- [24] G.B. Santos, A. Ganesan, F.S. Emery, Oral administration of peptide-based drugs: beyond lipinski's rule, *ChemMedChem* 11 (2016) 2245–2251, <https://doi.org/10.1002/cmdc.201600288>.
- [25] C.A. Lipinski, Rule of five in 2015 and beyond: target and ligand structural limitations, ligand chemistry structure and drug discovery project decisions, *Adv. Drug Deliv. Rev.* 101 (2016) 34–41, <https://doi.org/10.1016/j.addr.2016.04.029>.
- [26] B.C. Doak, B. Over, F. Giordanetto, J. Kihlberg, Oral druggable space beyond the rule of 5: insights from drugs and clinical candidates, *Chem. Biol.* 21 (2014) 1115–1142, <https://doi.org/10.1016/j.chembiol.2014.08.013>.
- [27] A. Capecchi, M. Awale, D. Probst, J.-L. Reymond, PubChem and ChEMBL beyond Lipinski, *Mol. Inform.* 38 (2019), e1900016, <https://doi.org/10.1002/minf.201900016>.
- [28] V. Jakob, S. Helmsing, M. Hust, M. Empting, Restriction-free construction of a phage-presented very short macrocyclic peptide library, *Methods Mol. Biol.* 2070 (2020) 95–113, [https://doi.org/10.1007/978-1-4939-9853-1\\_6](https://doi.org/10.1007/978-1-4939-9853-1_6).
- [29] J. Kügler, S. Wilke, D. Meier, F. Tomszak, A. Frenzel, T. Schirrmann, S. Dübel, H. Garritsen, B. Hock, L. Toleikis, M. Schütte, M. Hust, Generation and analysis of the improved human HAL9/10 antibody phage display libraries, *BMC Biotechnol.* 15 (2015) 10, <https://doi.org/10.1186/s12896-015-0125-0>.
- [30] S. Dübel, *Handbook of Therapeutic Antibodies*, secondnd ed., John Wiley & Sons Incorporated, Weinheim, 2014.
- [31] C.G. Ullman, L. Frigotto, R.N. Cooley, In vitro methods for peptide display and their applications, *Brief. Funct. Genomics* 10 (2011) 125–134, <https://doi.org/10.1093/bfpg/blr010>.
- [32] A. Frenzel, T. Schirrmann, M. Hust, Phage display-derived human antibodies in clinical development and therapy, *mAbs* 8 (2016) 1177–1194, <https://doi.org/10.1080/19420862.2016.1212149>.
- [33] S. Dübel, O. Stoevesandt, M.J. Taussig, M. Hust, Generating recombinant antibodies to the complete human proteome, *Trends Biotechnol.* 28 (2010) 333–339, <https://doi.org/10.1016/j.tibtech.2010.05.001>.
- [34] J. Kügler, J. Zantow, T. Meyer, M. Hust, Oligopeptide m13 phage display in pathogen research, *Viruses* 5 (2013) 2531–2545, <https://doi.org/10.3390/v5102531>.
- [35] V. Baeriswyl, C. Heinis, Phage selection of cyclic peptide antagonists with increased stability toward intestinal proteases, *Protein Eng. Des. Sel.* 26 (2013) 81–89, <https://doi.org/10.1093/protein/gzs085>.
- [36] N.B. Adey, A.H. Mataragnon, J.E. Rider, J.M. Carter, B.K. Kay, Characterization of phage that bind plastic from phage-displayed random peptide libraries, *Gene* 156 (1995) 27–31, [https://doi.org/10.1016/0378-1119\(95\)00058-E](https://doi.org/10.1016/0378-1119(95)00058-E).
- [37] M. Empting, O. Avrutina, R. Meusinger, S. Fabritz, M. Reinwarth, M. Biesalski, S. Voigt, G. Buntkowsky, H. Kolmar, Triazole bridge<sup>®</sup>: disulfide-bond replacement by ruthenium-catalyzed formation of 1,5-disubstituted 1,2,3-triazoles, *Angew. Chem. Int. Ed. Engl.* 50 (2011) 5207–5211, <https://doi.org/10.1002/anie.201008142>.
- [38] X. Jiang, X. Hao, L. Jing, G. Wu, D. Kang, X. Liu, P. Zhan, Recent applications of click chemistry in drug discovery, *Expet Opin. Drug Discov.* 14 (2019) 779–789, <https://doi.org/10.1080/17460441.2019.1614910>.
- [39] M. Roice, I. Johannsen, M. Meldal, High capacity poly(ethylene glycol) based amino polymers for peptide and organic synthesis, *QSAR Comb. Sci.* 23 (2004) 662–673, <https://doi.org/10.1002/qsar.200420021>.
- [40] G. Appendino, S. Bacchiega, A. Minassi, M.G. Cascio, L. De Petrocellis, V. Di Marzo, The 1,2,3-triazole ring as a peptido- and olefinomimetic element: discovery of click vanilloids and cannabinoids, *Angew. Chem.* 119 (2007) 9472–9475, <https://doi.org/10.1002/ange.200703590>.
- [41] S. Tomassi, A.M. Trotta, C. Ieranò, F. Merlino, A. Messere, G. Rea, F. Santoro, D. Brancaccio, A. Carotenuto, V.M. D'Amore, F.S. Di Leva, E. Novellino, S. Cosconati, L. Marinelli, S. Scala, S. Di Marco, Disulfide bond replacement with 1,4- and 1,5-disubstituted 1,2,3-triazole on C-X-C chemokine receptor type 4 (CXCR4) peptide ligands: small changes that make big differences, *Chemistry* 26 (2020) 10113–10125, <https://doi.org/10.1002/chem.202002468>.
- [42] S.R. Tala, A. Singh, C.J. Lensing, S.M. Schnell, K.T. Freeman, J.R. Rocca, C. Haskell-Luevano, 1,2,3-Triazole rings as a disulfide bond mimetic in chimeric AGRP-melanocortin peptides: design, synthesis, and functional characterization, *ACS Chem. Neurosci.* 9 (2018) 1001–1013, <https://doi.org/10.1021/acscchemneuro.7b00422>.
- [43] S. Pacifico, A. Kerckhoffs, A.J. Fallow, R.E. Foreman, R. Guerrini, J. McDonald, D.G. Lambert, A.G. Jamieson, Urotensin-II peptidomimetic incorporating a non-reducible 1,5-triazole disulfide bond reveals a pseudo-irreversible covalent binding mechanism to the urotensin G-protein coupled receptor, *Org. Biomol. Chem.* 15 (2017) 4704–4710, <https://doi.org/10.1039/C7OB00959C>.
- [44] A.M. White, S.J. de Veer, G. Wu, P.J. Harvey, K. Yap, G.J. King, J.E. Swedberg, C.K. Wang, R.H.P. Law, T. Durek, D.J. Craik, Application and structural analysis of triazole-bridged disulfide mimetics in cyclic peptides, *Angew. Chem. Int. Ed. Engl.* 59 (2020) 11273–11277, <https://doi.org/10.1002/anie.202003435>.
- [45] A.K. Heroven, K. Böhme, P. Dersch, The Csr/Rsm system of *Yersinia* and related pathogens: a post-transcriptional strategy for managing virulence, *RNA Biol.* 9 (2012) 379–391, <https://doi.org/10.4161/rna.19333>.
- [46] O. Duss, E. Michel, N. Diarra dit Konté, M. Schubert, F.H.-T. Allain, Molecular basis for the wide range of affinity found in Csr/Rsm protein-RNA recognition, *Nucleic Acids Res.* 42 (2014) 5332–5346, <https://doi.org/10.1093/nar/gku141>.